Applied Microbiology and Biotechnology (2024) 108:62
https://doi.org/10.1007/s00253-023-12853-1

BIOTECHNOLOGICAL PRODUCTS AND PROCESS ENGINEERING

The application of bacteria-derived dehydrogenases and oxidases in the synthesis of gold nanoparticles

Lela Martinaga[1] · Roland Ludwig[2] · Iva Rezić[1] · Martina Andlar[3,4] · Dietmar Pum[2] · Ana Vrsalović Presečki[5]

Received: 26 May 2023 / Revised: 22 September 2023 / Accepted: 3 October 2023

Abstract

In this work the green synthesis of gold nanoparticles (Au-NPs) using the oxidoreductive enzymes *Myriococcum thermophilum* cellobiose dehydrogenase (*Mt* CDH), *Glomerella cingulata* glucose dehydrogenase (*Gc* GDH), and *Aspergillus niger* glucose oxidase (*An* GOX)) as bioreductants was investigated. The influence of reaction conditions on the synthesis of Au-NPs was examined and optimised. The reaction kinetics and the influence of Au ions on the reaction rate were determined. Based on the kinetic study, the mechanism of Au-NP synthesis was proposed. The Au-NPs were characterized by UV–Vis spectroscopy and transmission electron microscopy (TEM). The surface plasmon resonance (SPR) absorption peaks of the Au-NPs synthesised with *Mt* CDH and *Gc* GDH were observed at 535 nm, indicating an average size of around 50 nm. According to the image analysis performed on a TEM micrograph, the Au-NPs synthesized with *Gc* GDH have a spherical shape with an average size of 2.83 and 6.63 nm after 24 and 48 h of the reaction, respectively.

Key points

- *The Au NPs were synthesised by the action of enzymes CDH and GDH.*
- *The synthesis of Au-NPs by CDH is related to the oxidation of cellobiose.*
- *The synthesis of Au-NPs by GDH was not driven by the reaction kinetic.*

Keywords Gold nanoparticles · Cellobiose dehydrogenase · Glucose dehydrogenase · Green synthesis · Kinetics

Introduction

Green nanoparticle synthesis is a fast-developing branch of nanotechnology that uses environmentally fiendly bioreductants for the synthesis of metallic NPs, ensuring a safe, environmentally friendly, simple, cost-effective and relatively reproducible process (Adelere and Lateef 2016). Bioreductants successfully used for the Au-NPs synthesis so far include: (i) agrowastes (grape waste, watermelon rind, palm oil mill effluent, eggshell membrane, etc.). (Adelere and Lateef 2016; Krishnaswamy et al. 2014; Patra and Baek 2015); (ii) plants, plant extracts, and algae (*Olax nana*, *Coriandrum sativum*, *Eucalyptus camaldulensis*, *Pelargonium roseum*, *Gracilaria crassa*, etc.) (Adelere and Lateef 2016; Kamaraj et al. 2022; Kuppusamy et al. 2016; Ovais et al. 2018c; Yadi et al. 2018); (iii) enzymes (sulphite reductase, disulphide reductase and keratinase, alcohol oxidase, serratiopeptidase, α-amylase, laccase, ligninase, urease, glucose oxidase, etc.) (Adelere and Lateef 2016; Ahmed et al. 2016a; Chinnadayyala et al. 2015; El-Batal et al. 2015; Faramarzi and Forootanfar 2011; Gholami-Shabani et al. 2015; Gour and Jain 2019; Gupta et al. 2015; Menon et al. 2017; Mishra and Sardar 2014; Muthurasu and Ganesh 2016; Ovais et al. 2018a; Ovais et al. 2018b; Rangnekar et al. 2007; Sanghi et al. 2011; Sharma et al.

✉ Ana Vrsalović Presečki
avrsalov@fkit.unizg.hr

Lela Martinaga
lela.pintaric@ttf.unizg.hr

1 Faculty of Textile Technology, University of Zagreb, Prilaz Baruna Filipovića 28a, 10000 Zagreb, Croatia

2 University of Natural Resources and Life Sciences, Gregor-Mendel-Straße 33, 1180 Vienna, Austria

3 Krka, d.d, Šmajerska Cesta 6, 8501 Novo Mesto, Slovenia

4 Faculty of Food Technology and Biotechnology, University of Zagreb, Pierottijeva Ulica 6, 10000 Zagreb, Croatia

5 University of Zagreb Faculty of Chemical Engineering and Technology, University of Zagreb, Savska Cesta 16/I, 10000 Zagreb, Croatia

Published online: 06 January 2024

2013; Venkatpurwar and Pokharkar 2010; Yasui and Kimizuka 2005). Agrowastes, plants and plant extracts are rich in various biomolecules (carbohydrates, flavonoids, alkaloids, phenols, proteins, steroids, tannins, etc.) that serve as reducing and/or stabilizing agents in the NP synthesis, while enzymes can act as catalysts for the formation of NP, release acids that act as reducing and stabilising agents, or serve as a reducing and capping agent themselves (Adelere and Lateef 2016). The use of enzymes, as a green synthesis method, has great potential to overcome the disadvantages of conventional chemical and physical synthesis of NPs, since enzymatic processes do not require the use of toxic chemicals and harsh reaction conditions, thus, reducing the negative impact on the environment (Adelere and Lateef 2016).

Nanotechnology is defined as the design, development, and application of materials, devices or other structures that have at least one dimension sized from 1 to 100 nm (Castro et al. 2014). Global production of engineered nanomaterials is rapidly increasing due to their specific properties differing from those of their bulk counterparts, enabling their application in various research area, as well as in numerous manufacturing processes and commercial products (Castro et al. 2014; Khan et al. 2017). Thus, noble metal nanoparticles (NPs) can have unique physical, chemical, and biological properties, including electronic and optical properties that are highly dependent on their size and shape, which determines their use in, i.e. health care, biomedicine, tissue engineering, gene delivery, drug delivery, food industry, space industry, optical devices, etc. (Ahmed et al. 2016a; Castro et al. 2014). Au-NPs are among the most important materials because of their long history of use and biocompatibility. The use of Au-NPs includes numerous applications such as biosensor, bioimaging, photothermal and anticancer therapy, targeted drug delivery, antimicrobial and antioxidant agents, of the cosmetic and textile industry products, food packaging, etc.

In this research, an enzyme-mediated synthesis of Au-NPs by *Myriococcum thermophilum* cellobiose dehydrogenase (*Mt* CDH), *Glomerella cingulata* glucose dehydrogenase (*Gc* GDH) and *Aspergillus niger* glucose oxidase (*An* GOX) was investigated and optimised and the synthesized NPs were characterised. The use of CDH and GDH for Au-NPs synthesis has not been reported yet, while the data for GOX are scarce (Muthurasu and Ganesh 2016; Yasui and Kimizuka 2005). To determine the mechanism of gold nanoparticle synthesis, a kinetic study was performed and a mathematical model was proposed. It allows us to reveal different mechanisms of nanoparticle synthesis by the action of these two enzymes. This type of study of the reaction mechanism of enzyme-mediated nanoparticle synthesis has not been proposed elsewhere.

Materials and methods

Materials

Gold(III) chloride trihydrate ($HAuCl_4 \cdot 3\ H_2O$), *D*-(+)-cellobiose, glucose oxidase from *Aspergillus niger* (Type VII-S, E.C. 1.1.3.4), citric and succinic acid were purchased from Sigma-Aldrich (USA), *D*-(+)-glucose, potassium dihydrogen phosphate, dipotassium hydrogen phosphate, and acetic acid from Carl Roth (Germany) and imidazole from PanReac AppliChem (Germany). All chemicals were of analytical reagent grade and were used without further purification. Milli-Q water (18.2 MΩ cm^{-1}, Millipore, Bedford, MA, USA) was used for the preparation of all buffer solutions. Cellobiose dehydrogenase from *Sclerotium rolfsii*, *Myriococcum thermophilum* and *Neurospora crassa*, and glucose dehydrogenase from *Glomerella cingulata* were provided by the Department of Food Science and Technology (University of Natural Resources and Life Sciences, Vienna, Austria). The cultivation of the organisms, enzymes separation and purification methods were described elsewhere (Harreither et al. 2011; Sygmund et al. 2011, 2012).

Carbohydrate driven synthesis of the Au-NPs

The reaction conditions under which the carbohydrate driven synthesis of Au-NPs occurred were explored. Two carbohydrates, cellobiose and glucose, in the concentration range of 0–5000 µM and 0–10000 µM, respectively, and a metal salt precursor, $HAuCl_4 \cdot 3\ H_2O$, in the concentration range of 0–1000 µM were used to design experiments with different initial reaction conditions. The impact of light, oxygen, and reaction medium (Milli-Q water, phosphate buffer pH 5.5 and pH 7, citrate buffer pH 4, pH 5.5 and pH 7, acetate buffer pH 4 and pH 5.5, imidazole buffer pH 5.5 and pH 7, succinate buffer pH 5.5) on the carbohydrate driven Au-NPs synthesis was also tested. All experiments were carried out in PVC 96 well plates and monitored visually (colour change) and by recording the spectra on Multimode Plate Reader EnSpire.

Determination of the optimal reaction conditions for the enzymatic synthesis

To determine the optimal reaction conditions for the enzymatic Au-NPs synthesis, different enzymes and their concentrations were tested. Reactions were carried out using cellobiose dehydrogenase (CDH) from three different sources (*Sclerotium rolfsii* (*Sr* CDH), *Myriococcum thermophilum* (*Mt* CDH) and *Neurospora crassa* (*Nc* CDH)) at concentrations of 0.01 and 1 mg cm^{-3} with 700 and 5000 µM of a

cellobiose as substrate and with 100, 550 and 1000 µM of a $HAuCl_4 \cdot 3\ H_2O$ as a metal salt precursor. Similary, reactions with the enzyme glucose dehydrogenase from *Glomerella cingulata* (*Gc* GDH) and glucose oxidase from *Aspergillus niger* (*An* GOX) were tested at concentrations of 0.1, 0.3 and 1 mg cm^{-3} with 1000 µM of glucose as a substrate and 550 µM of a $HAuCl_4 \cdot 3\ H_2O$ as a metal salt precursor. These experiments were carried out in 0.1 M imidazole and phosphate buffer both at pH 5.5 and 7 without oxygen and light in PVC 96 well plates. Nanoparticle formation was monitored visually (colour change) and by recording spectra on Multimode Plate Reader EnSpire.

The influence of temperature and stirring rate on an enzyme driven synthesis of the Au-NPs was examined in glass reactors (0.5 cm^3) and monitored for 72 and 24 h when performed with CDH and GDH, respectively.

Scaled-up enzymatic Au-NPs synthesis

Scaled-up experiments of the synthesis were done by the action of the enzymes *Mt* CDH and *Gc* GDH and were carried out in 10 cm^3 glass volumetric flasks at $T = 37$ °C without stirring and without oxygen and light in 0.1 M phosphate buffer pH 7 and 5.5, respectively. The enzyme and metal salt precursor ($HAuCl_4 \cdot 3\ H_2O$) concentration was 0.3 mg cm^{-3} and 550 µM, respectively, and was the same in both experiments. The cellobiose and glucose concentration was 700 and 1000 µM, respectively. Scaled-up experiments were monitored for 120 h in the case of Au-NP synthesis with *Mt* CDH and 48 h when *Gc* GDH was used.

Enzyme kinetics

The *Mt* CDH kinetics in the cellobiose and *Gc* GDH kinetics in the glucose oxidation were determined using the initial reaction rate method. Additionally, the impact of Au ions on the *Mt* CDH and *Gc* GDH activity was tested. Measurements were carried out in 0.1 M phosphate buffer pH 7 for *Mt* CDH and pH 5.5 for *Gc* GDH in a 2.5 cm^3 reactor at $T = 37$ °C, without stirring and without oxygen and light ($\gamma_{Mt\ \mathrm{CDH}} = 0.06$ mg cm^{-3}; $\gamma_{Gc\ \mathrm{GDH}} = 0.006$ mg cm^{-3}). The samples were taken during the first four hours of the reaction to determine the kinetics and during 28 h to determine the impact of Au ions on the reaction rate. In these measurements, glucose and cellobiose concentrations were followed by high performance liquid chromatography (HPLC).

Reactor experiments and model validation

The enzyme mediated synthesis of Au-NP was carried out in a 2.5 cm^3 glass batch reactor at $T = 37$ °C without stirring and without oxygen and light in 0.1 M phosphate buffer pH 7 for *Mt* CDH and pH 5.5 for *Gc* GDH. The metal salt precursor concentration ($HAuCl_4 \cdot 3\ H_2O$) was 550 µM while the enzyme concentration was 0.3 mg cm^{-3} and was the same in both experiments. The concentrations of cellobiose and glucose were 700 and 1000 µM, respectively. The addition of an enzyme to the reactor was considered to be the start of the reaction. The reactions were monitored by recording UV–VIS spectra, and sampling for the HPLC analysis was done at regular intervals during 168 h when *Mt* CDH was used and 144 h when *Gc* GDH was used for synthesis.

Mathematical model

The kinetics of cellobiose oxidation catalysed by *Mt* CDH and glucose oxidation catalysed by *Gc* GDH were described by single-substrate Michaelis–Menten kinetics with competitive inhibition by Au ions (Eqs. 1-2).

According to the reaction scheme (Fig. 1), the mass balance equations for the enzymatic synthesis of Au-NP with *Mt* CDH in a batch reactor were established (Eq. 3–5). The deactivation of *Mt* CDH was described using the first-order kinetics (Eq. 6).

$$r_{Au-cellobiose} = \frac{V_m^{cellobiose} \cdot c_{cellobiose}}{K_m^{cellobiose} \cdot \left(\frac{1+c_{Au^{3+}}}{K_i^{Au^{3+}}}\right) + c_{cellobiose}} \tag{1}$$

$$r_{Au-glucose} = \frac{V_m^{glucose} \cdot c_{glucose}}{K_m^{glucose} \cdot \left(\frac{1+c_{Au^{3+}}}{K_i^{Au^{3+}}}\right) + c_{glucose}} \tag{2}$$

$$\frac{dc_{cellobiose}}{dt} = -r_{Au-cellobiose} \tag{3}$$

$$\frac{dc_{Au^{3+}}}{dt} = -\frac{r_{Au-cellobiose}}{3} \tag{4}$$

$$\frac{dc_{Au-NPs}}{dt} = \frac{r_{Au-cellobiose}}{3} \tag{5}$$

$$\frac{dA_{MtCDH}}{dt} = -k_{d,MtCDH} \cdot A_{MtCDH} \tag{6}$$

The model parameters were estimated by nonlinear regression analysis using simplex or least squares method implemented in Scientist software, from experimental data, change of the initial reaction rate with a substrate concentration or from the reactor experiments. Standard deviations (σ) and the coefficient of determination (R^2) of the goodness-of-fit curve were also provided by Scientist (Vrsalović Presečki et al. 2018).

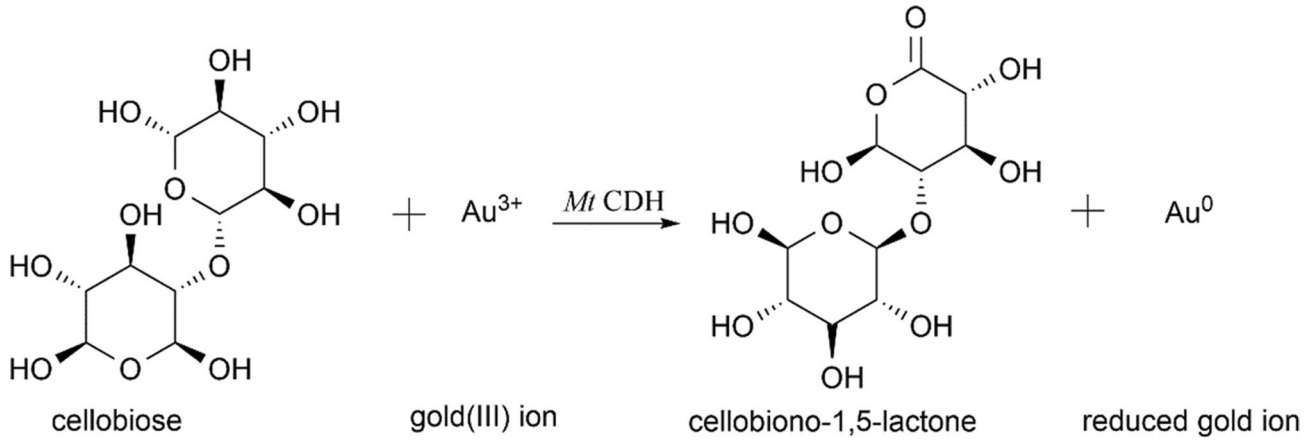

Fig. 1 Reaction scheme for cellobiose oxidation using *Mt* CDH

High performance liquid chromatography measurements

The *D*-(+)-cellobiose and *D*-(+)-glucose concentrations were measured by HPLC (Shimadzu, Japan) using a Carbohydrate Ca^{2+} Resin column (CS Chromatographie Service GmbH, 300 × 6.5 mm). The analysis was performed at 80 °C using a refractive index detector (RID). The isocratic method was used and the mobile phase was Milli-Q water with a flow rate of 0.8 cm^3 min^{-1}.

Ultraviolet–visible measurements

Ultraviolet–visible (UV–Vis) spectra during the investigation of carbohydrate driven Au-NPs, the screening of enzymes, the determination of optimal reaction conditions, performance of control experiments for the synthesis of Au-NPs driven by *Mt* CDH, and scaling-up the reactions were recorded using a Multimode Plate Reader EnSpire plate spectrophotometer (Perkin Elmer, USA) with samples contained in PVC 96 well plates, operating at a 5 nm resolution from 300 to 750 nm. During control experiments for the synthesis of Au-NP driven by *Gc* GDH and model validation, UV–Vis spectra were recorded using a Shimadzu UV-1800 spectrophotometer (Shimadzu, Japan), with samples measured from 300 to 700 nm in a quartz cuvette with a resolution of 1 nm.

Transmission electron microscopy analysis

Samples for transmission electron microscope (TEM) analysis were taken from the reactor during the 48 h of Au-NPs synthesis when *Gc* GDH was used and were centrifuged. The synthesised Au-NPs were washed three times in Milli-Q water and frozen. In sample preparation for TEM characterisation, a drop of the Au-NPs resuspended in Milli-Q water was placed on a carbon-coated copper grid and dried at room temperature. The TEM study was performed on a FEI Tecnai G^2 Spirit instrument (Thermofisher Scientific, Eindhoven, The Netherlands) operated at 160 kV.

Results

Carbohydrate driven synthesis of the Au-NPs

The addition of various carbohydrates such as galactose, glucose, fructose, maltose and sucrose (as functional compounds consisting of hydroxyl groups and hemiacetal reducing end) to the reaction solution containing precursor salts of gold (Au) could result in the formation of Au-NPs (Park et al. 2011). Considering that the main objective of this research was to synthesize Au-NPs by the actions of the enzymes CDH, GDH, and GOX,, the possible reaction between carbohydrate and Au salt was preliminarily investigated to avoid carbohydrate driven synthesis.

The experiments in 0.1 M phosphate buffer (pH 7) containing different concentrations of cellobiose (0–5000 µM) and Au ions (0–10000 µM) has shown that carbohydrate-driven Au-NP synthesis occurred at cellobiose concentrations greater than 700 µM and Au ions in the range of 100 to 625 µM (Fig. S1). In experiments with glucose (0–10000 µM) and Au ions, the carbohydrate driven synthesis also occurred as expected and was pronounced at glucose concentrations greater than 1000 µM and Au ions in the range of 100 to 1000 µM (Engelbrekt et al. 2009). At the higher substrate and Au ions concentrations, the colour change indicated that some reaction took place, but according to the UV–Vis spectra, no spherical Au-NPs were formed. It can be assumed that the particles agglomerated and/or were shaped differently and therefore shifted SPR absorption peak at longer wavelengths outside the monitored

range. The spectra of the described reactions resulted with peaks around 590 nm and 555 nm for cellobiose and glucose, respectively (Fig. S2a and b). According to the literature, the peaks around 555 nm correspond to the Au-NP size of 80 nm while the peaks at the longer wavelength (590 nm) indicate the SPR feature of the aggregated Au-NPs (Xu et al. 2018).

The impact of light, oxygen, and reaction medium (water and phosphate buffer pH 7) on carbohydrate Au-NPs synthesis was further examined using glucose as a referent substrate at concentrations of 1000 and 10000 µM and Au ions in the range of 100 to 1000 µM (Fig. S3). Based on visual observations, it was concluded that fewer particles (less colouration) were formed in experiments conducted without light and without oxygen, as well as in reactions in water. However, because enzymes will be further employed for the reaction and to avoid carbohydrate driven synthesis as much as possible, it was decided to run future experiments without oxygen and light, but in an appropriate buffer. Therefore, five buffers with different pH values were tested (phosphate buffer pH 5.5 and pH 7, citrate buffer pH 4, pH 5.5 and pH 7, acetate buffer pH 4 and pH 5.4, imidazole buffer pH 5.5 and pH 7, succinate buffer pH 5.5). The results revealed that carbohydrate driven Au-NPs synthesis did not occur in 0.1 M imidazole and phosphate buffer at pH 5.5 and 7 at glucose concentration of 1000 µM (Fig. S4).

Screening of enzymes and reaction conditions for the synthesis of Au-NPs

Cellobiose dehydrogenase (CDH) from three different sources (*Sclerotium rolfsii* (*Sr* CDH), *Myriococcum thermophilum* (*Mt* CDH), *Neurospora crassa* (*Nc* CDH), glucose dehydrogenase from *Glomerella cingulata* (*Gc* GDH) and glucose oxidase from *Aspergillus niger* (*An* GOX) were examined for the synthesis of Au-NPs at different reaction conditions (enzyme, substrate, and Au ions concentration, buffer, stirring, and temperature). To avoid carbohydrate driven Au-NPs synthesis, experiments were conducted without light and oxygen and in phosphate or imidazole buffer.

To determine the appropriate reaction conditions, various concentrations of cellobiose dehydrogenases (0.01 and 1 mg cm^{-3}) and Au ions (100 and 550 µM) in 0.1 M imidazole and phosphate buffer (pH 5.5 and 7 each; Fig. S5) were examined. At a lower CDH concentration (0.01 mg cm^{-3}) no Au-NPs synthesis occurred. The results obtained at a higher enzyme concentration (1 mg cm^{-3}) are shown in Fig. 2. Approximately the same Au-NPs formation was observed by *Mt* CDH in all buffers, *Sr* CDH in phosphate buffer pH 5.5 and *Nc* CDH in imidazole buffer pH 7 Since the highest amount of NPs was obtained by *Mt* CDH in 0.1 M phosphate buffer pH 7 and Au ions concentration of 550 µM, these conditions were used for further tests. In addition, three

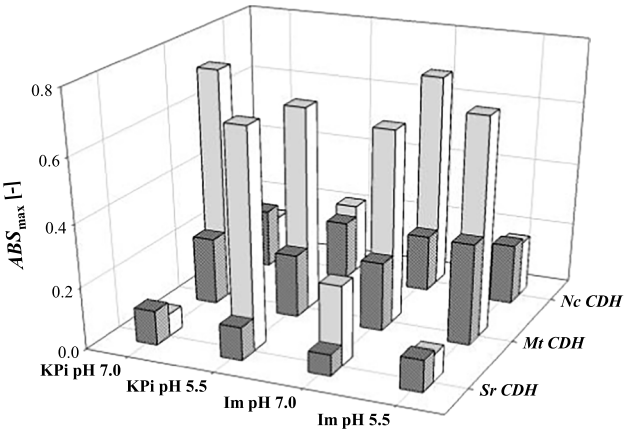

Fig. 2 Effect of different buffers and Au^{3+} concentration on *Sr* CDH, *Mt* CDH and *Nc* CDH driven Au-NPs synthesis (without light, without oxygen and stirring, 0.1 M phosphate and imidazole buffer pH 5.5 and 7, $c_{cellobiose} = 700$ µM, $c_{Au3+} = 100$ (dark bars); 550 µM (white bars), $\gamma_{CDH} = 1$ mg $cm.^{-3}$)

concentrations of *Mt* CDH (0.1, 0.3 and 1 mg cm^{-3}) were tested for the synthesis of Au-NPs. According to the maximal absorbances (data not shown), almost the same results were obtained when 0.3 and 1 mg cm^{-3} *Mt* CDH were used. Therefore, the enzyme concentration 0.3 mg cm^{-3} was used for the further experiments.

The influence of temperature (room temperature and $T = 37$ °C) and stirring rate (without stirring and stirring on a rotator (20 rpm)) on Au-NPs synthesis was examined at previously determined optimal reaction conditions (0.3 mg cm^{-3} *Mt* CDH, 550 µM $HAuCl_4 \cdot 3\ H_2O$, 700 µM cellobiose, 0.1 M phosphate buffer pH 7, without light and oxygen). The experiments on the rotator were carried out in triplicate and the reaction was monitored for 72 h. The absorption spectrums measured at the end of the reactions are shown in Fig. S6, while the maximum absorbance obtained are given in Table 1. Since maximum absorbance during Au-NPs synthesis were observed at room temperature at 540 nm and at $T = 37$ °C at 535 nm, it can be assumed that NPs of similar size were synthesized. The highest amount of NPs with *Mt* CDH was achieved, at $T = 37$ °C and without stirring and these conditions were applied in further experiments.

Preliminary experiments with *Gc* GDH and *An* GOX were performed with three enzyme concentrations (0.1, 0.3 and 1 mg cm^{-3}) and constant concentrations of glucose (1000 µM) and Au ions (550 µM) in 0.1 M imidazole and phosphate buffer pH 5.5 and 7 each (Fig. S7). Although it was previously shown that it is possible to synthesize Au-NPs with the GOX enzyme, this did not occur under the above conditions (Muthurasu and Ganesh 2016; Yasui and Kimizuka 2005). Namely, to avoid carbohydrate driven synthesis of Au-NPs the reactions were performed without

Table 1 Maximum absorbance obtained during *Mt* CDH driven Au-NPs synthesis at room temperature and at $T = 37$ °C with and without stirring

Experiment	ROOM TEMPERATURE		$T = 37$ °C	
Time	ABS_{max} [-]		ABS_{max} [-]	
	Without stirring	With stirring*	Without stirring	With stirring*
Beginning	0.024	-	0.022	-
After 24 h	0.099	0.125 ± 0.01347	0.261	0.262 ± 0.01014
After 48 h	0.176	0.198 ± 0.01406	0.567	0.360 ± 0.02449
After 72 h	0.234	0.218 ± 0.01189	0.755	0.505 ± 0.01975

*mean value of three measurements

oxygen and at low glucose concentration. With respect to the gathered results, the Au-NPs formation by *An* GOX was not further investigated.

The formation of Au-NPs by *Gc* GDH occurred in phosphate buffer pH 5.5 and 7 which was not the case in imidazole buffer at both tested pH values. The maximum absorbance shown in Fig. 3 indicates that more Au-NPs were formed in phosphate buffer pH 5.5 (light grey bars). Enzyme concentration did not significantly affect Au-NPs formation. Therefore, further experiments were carried out at a *Gc* GDH concentration of 0.3 mg cm^{-3} in phosphate buffer pH 5.5.

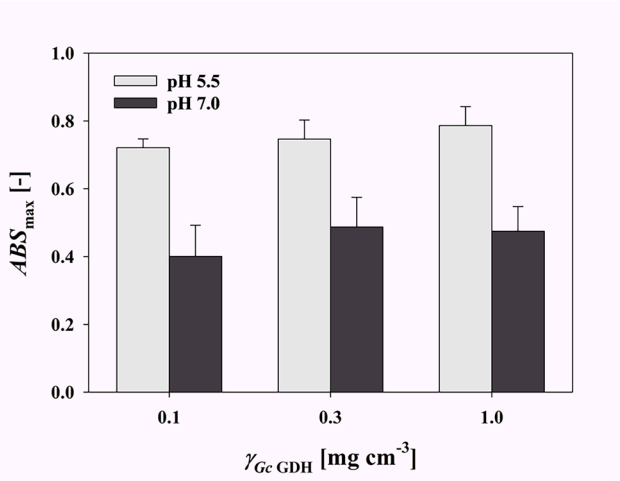

Fig. 3 Maximum absorbance of Au-NPs synthesized with *Gc* GDH (without light, without oxygen, 0.1 M phosphate buffer pH 5.5 (light bars) and pH 7 (dark bars), $c_{glucose} = 1000$ µM, $c_{Au3+} = 550$ µM, $\gamma_{Gc\ GDH} = 0.1/0.3/1$ mg $cm.^{-3}$)

The impact of temperature and stirring on Au-NPs synthesis when *Gc* GDH employed was studied analogously to the experiments with *Mt* CDH, but in this case the reaction was monitored for 24 h. The results are given in Table 2 Therefore, further experiments were conducted with *Gc* GDH at $T = 37$ °C and without stirring.

Scaled-up experiments

Scaled-up synthesis of Au-NPs by the action of the enzymes *Mt* CDH and *Gc* GDH was scaled to a volume of 10 cm^3 and performed under most appropriate reaction conditions for each enzyme as previously determined. The maximum absorbance obtained after 72 h of reaction with *Mt* CDH was 0.705 (at 540 nm; Fig. S8c).

The synthesis of Au-NPs by the action of enzyme *Gc* GDH was monitored for 48 h and the maximum absorbance measured after 24 h of reaction was 0.696 (at 525–530 nm; Fig. S8d).

Enzyme kinetics

The *Mt* CDH and *Gc* GDH kinetics in the oxidation reaction of cellobiose and glucose, respectively, were measured by the initial reaction rate method and described by single-substrate Michaelis–Menten kinetics. Maximal activities and Michaelis constants for cellobiose and glucose were estimated from experimental data (Table 3). Impact of the

Table 2 Maximum absorbance obtained during *Gc* GDH driven Au-NPs synthesis at room temperature and at $T = 37$ °C with and without stirring

Experiment	ROOM TEMPERATURE		$T = 37$ °C	
Time	ABS_{max} [-]		ABS_{max} [-]	
	Without stirring	With stirring*	Without stirring	With stirring*
Beginning	0.022	0.022 ± 0.00309	0.022	0.020 ± 0.00262
After 6 h	0.408	0.503 ± 0.00974	0.638	0.637 ± 0.01929
After 24 h	0.686	0.629 ± 0.03549	0.810	0.817 ± 0.04000

*mean value of three measurements data (Table 3)

Table 3 Kinetic parameters of *Mt* CDH and *Gc* GDH catalysed oxidation of cellulose and glucose

Parameter	Value	
	Mt CDH	*Gc* GDH
V_m [U mg^{-1}]	0.0557	0.6118
K_m [mmol dm^{-3}]	0.7736	0.6901
K_i [mmol dm^{-3}]	$1.71 \cdot 10^{-3}$	$4.17 \cdot 10^{-5}$

Au ions on the reaction kinetics was also investigated and it was found out that it decreases the reaction rates of both enzymes. The inhibitions were described by the Michaelis–Menten equation with competitive product inhibition (Eqs. 1–2) and the inhibition constants were estimated from the experimental.

Reactor experiment and model validation

The synthesis of gold nanoparticles was carried out in a batch reactor by the action of *Mt* CDH and *Gc* GDH using cellobiose and glucose as substrate, respectively. In order to examine the influence of reaction kinetics on formation of Au-NPs, carbohydrate concentrations were monitored in these experiments in addition to maximal absorbance. The reactions were carried out under the previously determined optimal reaction conditions.

The results of Au-NPs synthesis using the enzyme *Mt* CDH are shown in Fig. 4 as the change in maximum absorbance (at 530–540 nm) and cellobiose concentration during the reaction time. A very good correlation was observed between the experimental data and the data obtained by the model simulation (*Chapter Mathematical model*, $R^2 = 0.99$; $\sigma = 0.08$), that is, the mathematical model was validated. Additionally, a correlation was observed between the increase in maximum absorbance (Au-NPs concentration simulated by the model was multiplied by estimated extinction coefficient, $\varepsilon = 5.4267$ mM^{-1}) and the decrease in cellobiose concentration. During the experiment, the *Mt* CDH deactivation was noticed and was described by first-order kinetics (Eq. 6). The deactivation rate was estimated based on the experimental data – $k_d = 0.00019$ min^{-1}.

In contrast, the results of an experiment in which Au-NPs were synthesized by *Gc* GDH (Fig. 5) did not show the correlation between the Au-NPs synthesis and glucose oxidation, as no change in glucose concentration was observed during the reaction.

TEM characterization

TEM images (Fig. 6a and b) and especially the quantitative determination of the size of the nanoparticles (Fig. 6c and d) showed that the particles agglomerated and increased over time (average size of 2.83 ± 2.40 and 6.63 ± 3.03 nm after 24 and 48 h, respectively).

Discussion

The aim of this work was to examine the possibilities of synthesis of Au-NPs by the action of oxidoreductases, which provide electrons for the reduction of the metal ions by oxidising the substrate. The oxidoreductases studied catalyse carbohydrate oxidation reactions, which themselves can

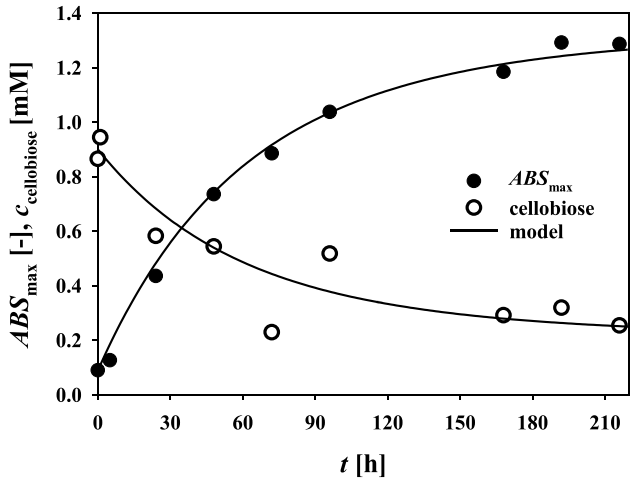

Fig. 4 Validation of the mathematical model for *Mt* CDH driven Au-NPs synthesis ($V = 3.5$ cm^3, without light, oxygen and stirring, 0.1 M phosphate buffer pH 7, $T = 37$ °C, $c_{cellobiose} = 700$ µM, $\gamma_{Mt\ CDH} = 0.3$ mg cm.$^{-3}$, $c_{Au3+} = 550$ µM)

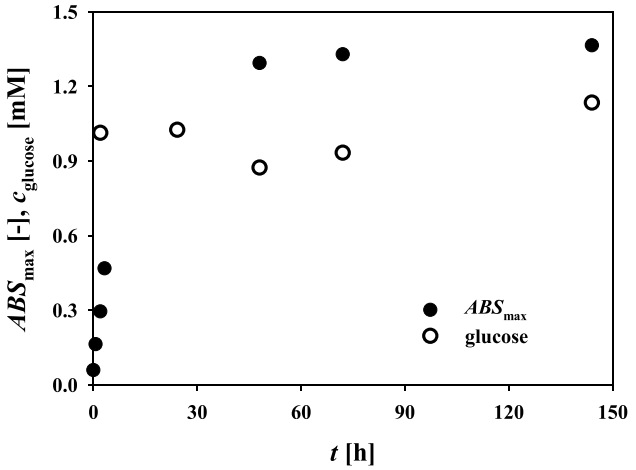

Fig. 5 Results of the *Gc* GDH driven Au-NPs synthesis showing that glucose oxidation and Au-NPs formation are unrelated ($V = 2.5$ cm^3, without light, oxygen and stirring, 0.1 M phosphate buffer pH 5.5, $T = 37$ °C, $c_{glucose} = 1000$ µM, $\gamma_{Gc\ GDH} = 0.3$ mg cm.$^{-3}$, $c_{Au3+} = 550$ µM)

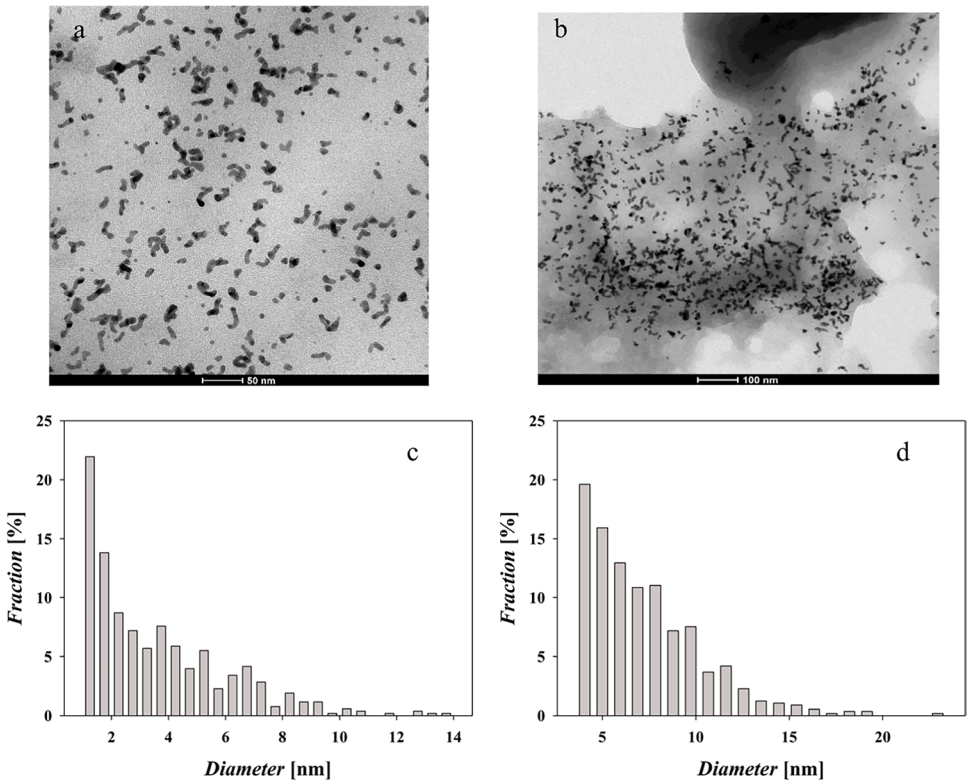

Fig. 6 Results of the TEM analysis of gold nanoparticles synthesized using *Gc* GDH: a and c – after 24 h; b and d – after 48 h ($V = 10$ cm^3, without light, oxygen and stirring, 0.1 M phosphate buffer pH 5.5, $T = 37$ °C, $c_{glucose} = 1000$ µM, $\gamma_{Mt\ CDH} = 0.3$ mg cm.$^{-3}$, $c_{Au3+} = 550$ µM)

serve as Au ion reductants. (Park et al. 2011). The carbohydrates used with the enzymes investigated in this work are cellobiose and glucose. To the best of our knowledge, Au-NPs formation using cellobiose as a reducing agent has not yet been reported. Scampicchio et al. (2009) observed Au-NP formation by addition of galactose, glucose, fructose, maltose and sucrose to the reaction solution containing HAuCl4 · 3 H2O and a surfactant in alkaline media, thus demonstrating the ability of these compounds to reduce Au(III) to Au(0). Castro-Guerrero et al. (2018) used fructose and citric acid as reducing and stabilising agents, and as a co-reducing agents for Au-NP synthesis, resulting in spherical NPs with an average diameter of 12 nm. Successful synthesis of Au-NPs using purified bacterial exopolysaccharide (consisting mainly of glucose and galactose), hyaluronic acid, cellulose dextran, alginic acid and chitosan as reducing and/or stabilising agents was also reported (Huang and Yang 2004; Park et al. 2011; Sathiyanarayanan et al. 2014). Suvarna et al. (2017) used glucose for the same purpose, while Engelbrekt et al. (2009) used glucose and starch for the synthesis of spherical Au-NP with an average diameter of 13 and 4 nm when the synthesis was carried out in phosphate and MES (2-(N-morpholino)ethanesulfonic acid) buffers, respectively. The latter research indicates the importance of the chemical nature of the buffers as one of the key factors for the formation of Au-NPs. In addition to the chemical nature, the pH of the buffer, the concentration of the reducing agent and the metal precursor, the temperature and the incubation time are also among the most important reaction parameters directly affecting the shape, size and homogeneity of the synthesised NPs (Ahmed et al. 2016b; Engelbrekt et al. 2009; Jalani et al. 2018; Patra and Baek 2014; Shervani and Yamamoto 2011). Harada and Kizaki (2016) found that photoreduction has a major impact on the formation of Au nanoparticles in an aqueous ethanol solution of a polymer and is involved in the successive stages of reduction – nucleation, autocatalytic surface growth on nucleates, aggregative growth and aggregation/precipitation process. Sylvestre et al. (2004) reported that the oxygen present in water leads to partial oxidation of the synthesised gold nanoparticles, which eventually increases their chemical reactivity and has a great influence on their growth.

Therefore, preliminary experiments were carried out with enzyme substrates (cellobiose and glucose) and Au ions and the impact of light, oxygen, and reaction medium was examined to find suitable conditions under which carbohydrate driven synthesis will be avoided. UV–vis spectra were measured to confirm the Au-NP formation, taking into account their characteristic absorption spectrum and absorption band around 520 nm, which is related to the surface plasmon resonance (SPR) of Au-NPs (Huang and El-Sayed 2010). The position and width of the SPR absorption peak are strongly dependent on both the size and shape of the Au-NPs. A shift to longer wavelengths and a broadening of the SPR peak was observed with an increase in Au-NP size and a decrease in the distance between the particles due to their

aggregation (Zuber et al. 2016). Zuber et al. (2016) and He et al. (2005) reported that the intensity of the SPR band was related to the concentration of Au-NPs and showed that the peak maximum shifted from 514 to 526 nm and from 520 to 530 nm for Au-NPs of 5 and 50 nm and 12 to 41 nm in diameter, respectively. With the further increment of the Au-NP size to 100 nm, the peak maximum is expected to shift to 572 nm. Shi et al. (2012) showed that rod-shaped Au-NPs have two bands in the absorption spectrum. The lower peak near 520 nm represents the SPR along the transverse direction, while the dominant peak arises from the SPR along the longitudinal direction and was shifted to the near-infrared (NIR) region from 650 to 1050 nm (Shi et al. 2012).

The performed experiments showed that carbohydrate driven synthesis occurred in the presence of high concentrations of cellobiose ($c > 700$ µM) and glucose ($c > 1000$ µM), as well as at high Au ion concentration (Fig. S1). It was found that, the carbohydrate-driven synthesis by glucose resulted in the smaller NPs according to the maximum absorbance peak (Fig. S2). Investigation of the impact of light and oxygen on the synthesis of NPs by glucose showed that they both had a positive influence (Fig. S4). Thus, to avoid carbohydrate driven synthesis, the experiments with the enzymes are performed in the dark and without oxygen. The synthesis of Au-NPs by glucose was p carried out in water and different buffers (Fig. S3 and S4). The impact of the reaction medium was evident and the citrate buffers (pH 4, 5.5 and 7), acetate (pH 5.5) and succinate (pH 5.5) were those that promoted the synthesis even at low glucose concentration (1000 µM). NPs synthesis did not occur in water and other buffers (phosphate pH 5.5. and 7, acetate pH 4 and imidazole pH 5.5 and 7) at a lower glucose concentration.

Enzymes are considered as the preferred bioreductants for the green synthesis of Au-NPs of different sizes and shapes. The use of various extracellular and intracellular bioreducing microbial enzymes has already resulted in mostly spherical, but also hexagonal, triangular, octahedral, polygonal, planar and cubic Au-NPs with sizes in the range of 8–70 nm (Ovais et al. 2018a). For instance, the α-NADPH-dependent sulphite reductase was used for the synthesis of spherical Au-NPs with a size of 7–20 nm, the enzyme laccase from *Paraconiothyrium variabile* and *Pleurotus ostreatus* was used for the synthesis of Au-NPs with a size of 71–266 nm and 22–39 nm, respectively, while the use of laccase and ligninase in combination resulted in a spherical Au-NPs with a size of 10–100 nm (El-Batal et al. 2015; Faramarzi and Forootanfar 2011; Gholami-Shabani et al. 2015; Sanghi et al. 2011). For the same purpose, Chinnadayyala et al. (2015) reported the use of alcohol oxidase and Venkatpurwar and Pokharkar (2010) of serratiopeptidase enzyme. Mishra and Sardar (2014) and Rangnekar et al. (2007) reported the use of the enzyme α-amylase and Sharma et al. (2013) used urease as both reducing and stabilising agent for the synthesis of Au-NP.

The oxidoreductase glucose oxidase from *Aspergillus niger* (*An* GOX) was also reported as suitable for the reduction and stabilization of Au(III) ions in the presence of *β-D*-glucose and glucose with sodium metal addition as this enzyme is able to perform direct electron transfer (DET) of two electrons through its flavin adenine dinucleotide (FAD) part. The synthesized Au-NPs were stable and had an average size of 14.5 and 5.4 nm when *β-D*-glucose and glucose with sodium metal addition were used, respectively (Muthurasu and Ganesh 2016; Yasui and Kimizuka 2005). However, the influence of the various reaction parameters on the characteristics of the synthesised NPs remained unknown. The enzyme cellobiose dehydrogenase, also from the family of oxidoreductases, consists dehydrogenase domain (DH) with FAD as the prosthetic group, and a *b*-type heme-containing cytochrome domain (CYT), connected via the linker region (Malel et al. 2010; Wang et al. 2012). The ability to perform internal electron transfer (IET) from the FAD to the CYT domain and DET of electrons from the oxidation of its natural substrate (cellobiose) to a certain electron acceptor i.e. gold electrode, is being investigated for the development of biosensors and enzymatic biofuel cells (Ma and Ludwig 2019; Tavahodi et al. 2017). Malel et al. (2010) explored DET and mediated electron transfer (MET) using benzoquinone/hydroquinone as mediators and Au seeds as catalysts for Au-NPs reduction. This research showed that these processes are pH dependent and resulted with relatively large Au-NPs. Therefore, more information about the process is still needed. Glucose dehydrogenase from *Glomerella cingulata* is another FAD-dependent oxidoreductive enzyme capable of performing electron transfer that has been studied by several research groups (Muguruma et al. 2017; Zafar et al. 2012). As far as we know, there are no reports on the use of this enzyme as a reducing agent for the synthesis of Au-NPs.

Three types of oxidoreductases, cellobiose dehydrogenase (CDH), glucose dehydrogenase from *Glomerella cingulata* (*Gc* GDH) and glucose oxidase from *Aspergillus niger* (*An* GOX) were employed in this work. Also for CDH, the enzymes from thee different sources were investigated: *Sclerotium rolfsii* (*Sr* CDH), *Myriococcum thermophilum* (*Mt* CDH) and *Neurospora crassa* (*Nc* CDH). To optimize the NPs production, the impact of reaction conditions on NPs synthesis was examined. These investigations were performed without light and oxygen and in phosphate or imidazole buffer to minimize the effects of carbohydrate driven Au-NPs synthesis.

The experimental data showed that of the CDHs tested, *Mt* CDH in phosphate buffer pH 7 at an enzyme concentration of 0.3 mg cm^{-3} and the Au ion concentration of 550 µM resulted in the highest NP formation (Fig. 2). CDH consists of a dehydrogenase domain (DH) carrying flavin adenine dinucleotide (FAD) and a cytochrome domain (CYT) connected by a flexible linker region (Malel et al. 2010; Tavahodi et al. 2017). To find out which domain is crucial for

Au-NPs formation, experiments were conducted at a previously defined substrate and Au ions concentration with *Mt* CDH, bovine serum albumin (BSA) as control protein, isolated CYT, and two types of DH domain. The results showed (Fig. S9) a low Au-NPs formation in the presence of DH domain (Fig S9 d and e) and an absence of the same in the presence of the other proteins examined (Fig S9 b and c). It was concluded that none of the domains is individually responsible for NPs synthesis, but their interaction. Likewise, possible Au-NPs synthesis was examined in the reaction without cellobiose (only Au ions and *Mt*CDH) (Fig. S9g) and without the enzyme (only cellobiose and Au ions) (Fig. S9f), and in both cases no Au-NPs formation was observed.

The reaction temperature is one of the reaction conditions that play an important role in NPs synthesis. While various physical and chemical methods require high temperatures (even above 350 °C), the synthesis of NPs with bioreductants can be achieved at temperatures below 100 °C or at room temperature (Jalani et al. 2018; Patra and Baek 2014). It has been reported that regardless of the method used for synthesis, temperature directly affects reaction rate, size, shape, morphology and final properties of the synthesized NPs and therefore needs to be optimized for a single process (Iravani and Zolfaghari 2013; Khalilzadeh and Borzoo 2016; Kumari et al. 2016; Mountrichas et al. 2014; Rajeshkumar et al. 2017). For instance, Iravani and Zolfaghari (2013) and Rajeshkumar et al. (2017) reported that higher reaction temperatures resulted in smaller NPs. Khalilzadeh and Borzoo (2016) and Mountrichas et al. (2014) observed that the reaction rate decreases with decreasing temperature in NPs synthesis and vice versa by, while the dependence of NPs shape on reaction temperature and pH of the reaction medium was determined in the work of Kumari et al. (2016). Ahmad et al. (2006) reported that stirring can also affect NPs production by enzymes and proteins (responsible for reduction) in the reaction medium.

Accordingly, the influence of temperature (room temperature and $T = 37$ °C) and stirring (without stirring and stirring on a rotator at 20 rpm) on Au-NPs synthesis by *Mt* CDH was examined (Table 1, Fig. S6). Based on the values of the maximum absorbance, it can be concluded that more Au-NPs were formed at higher tested temperature, which was expected considering reduced diffusion effect and thus higher reaction rate at elevated temperatures (Khalilzadeh and Borzoo 2016; Mountrichas et al. 2014). The effect of stirring at room temperature was insignificant, and this can be explained by lower enzyme deactivation and lower release of proteins/amino acids at lower temperatures. At higher tested temperatures, the difference between the maximum absorbance with and without stirring during the reaction was more pronounced. More Au-NPs formed in the reaction without stirring may be the result of more enzyme (amino acids that build the enzyme) available and released into the reaction medium under stationary conditions than under stirring conditions as was found in the literature (Ahmad et al. 2006). Therefore, further experiments with *Mt* CDH were performed at $T = 37$ °C and without stirring.

The same investigations as for CDH were performed with GDH and GOX (Fig. S7). Although it has previously been shown that it is possible to synthesize Au-NPs with the GOX enzyme (Muthurasu and Ganesh 2016; Yasui and Kimizuka 2005), this was not the case under the conditions chosen to eliminate carbohydrate driven synthesis. Therefore, the study of Au-NPs synthesis with GOX was not further performed. The tests with the *Gc* GDH revealed that the Au-NPs were successfully formed in the 0.1 M phosphate buffer pH 5.5 at an enzyme concentration of 0.3 mg cm^{-3} and the Au ion concentration of 550 µM (Fig. S7, Fig. 3). Investigation of the impact of temperature and stirring on Au-NPs synthesis by *Gc* GDH (Table 2) revealed that the influence of stirring on Au-NPs formation was less significant when *Gc* GDH was used compared to *Mt* CDH driven Au-NPs synthesis (Table 1). As in the case of *Mt* CDH, higher tested temperature resulted in enhanced Au-NPs formation, confirming a lower diffusion effect at higher temperature. Since the maximum absorbance of the synthesised Au-NPs were obtained at 540–550 and 525–530 nm (data not shown) during the reaction carried out at room temperature and $T = 37$ °C, respectively, smaller NPs are expected at higher tested temperatures. The obtained results suggested that it is optimal to carry out Au-NPs synthesis by *Gc* GDH at $T = 37$ °C and without stirring.

Scale-up experiments were performed in a volume of 10 cm^3, which corresponds to a 20-fold magnification compared to the volume of the test experiments (Fig. S8). Scaled-up synthesis of Au-NPs by the *Mt* CDH resulted with the maximum absorbance of 0.705 (at 540 nm; Fig. S8c) which was in good correlation with the maximum absorbance obtained at the same reaction time in a preliminary experiment in a reactor of 0.5 cm^3 (Table 1, $ABS_{max} = 0.755$ at 535 nm). This indicates that Au-NPs synthesis by *Mt* CDH is reproducible on a larger scale under the optimal reaction conditions. Upscaling the process was not so successful in the case of *Gc GDH*. Obtained maximal absorbance of 0.696 (at 525–530 nm; Fig. S8d) corresponds to a 10% lower Au-NPs production compared to 0.810 (at 530–535 nm) obtained at a volume of 0.5 cm^3 (Table 2).

A kinetic study of the *Mt* CDH and *Gc* GDH together with the proposed model (*Chapter Mathematical model*) was performed to investigate whether is the rate of the Au-NPs formation related to the reaction performed by examined enzymes. The kinetics of both enzymes were examined in the reaction of the corresponding carbohydrate oxidation by initial reaction rate method. In addition, the impact of Au ions on the reaction rate was measured. The values of

Michaelis constants are similar, and thus both enzymes have similar substrate specificity. The maximal activity of *Gc* GDH is higher, and therefore, glucose oxidation is faster than cellobiose oxidation. Furthermore, the impact of different Au ions on both enzyme activities was examined (Table 3). The obtained data indicated that the increased Au ions concentration led to a decrease in enzymes activities and the reactions were described by single-substrate Michaelis–Menten kinetics with competitive inhibition by Au ions. Based on the estimated inhibition constants (Table 3), it was found that Au ions slightly inhibit the cellobiose oxidation while the inhibition of glucose oxidation is significantly higher.

Using the kinetic data, the mathematical model (*Chapter Mathematical model*) was validated in the batch reactor. For the enzyme *Mt* CDH, results obtained by model simulation were in very good agreement with the experimental data (Fig. 4). This suggests that the mechanism of formation of Au NPs with the *Mt* CDH enzyme is directly related to the kinetics of cellobiose oxidation, i.e. reduction of Au ions, as shown in Fig. 1. This was also proven by the control experiments mentioned previously in which single impact of *Mt* CDH and cellobiose on Au ion reduction was examined (Fig. S9 f and g).

This was not the case for the *Gc* GDH enzyme in the reaction of glucose oxidation, which was proved to be significantly inhibited by Au ions (Fig. 5, Table 3). In order to reveal the mechanism of NPs formation for this enzyme, control experiments for the formation of Au-NPs were performed in the following combinations: *Gc* GDH + glucose + Au^{3+}, *Gc* GDH + Au^{3+}, and glucose + Au^{3+} (Fig. S10). Based on the maximum absorbances, reaction rate was estimated from the first four hours of reaction. From the results, it was concluded that the synthesis of Au-NPs by *Gc* GDH occurs due to the reduction of Au ions along with glucose and amino acids, which are an integral part of the enzyme (Coronato Courrol and de Matos 2016; Engelbrekt et al. 2009; Maruyama et al. 2015). The final amount of Au-NPs obtained after 120 h is approximately the same regardless of the presence of glucose, as it is determined by the initial concentration of Au ions in the solution. However, the estimated reaction rate of these separate reactions is lower than in the case when enzyme and substrate were used together for Au-NPs synthesis, implying that *Gc* GDH and glucose in synergy have a positive effect on the formation rate of Au-NPs.

TEM measurements showed that the average size of the Au-NPs synthesised with *Gc* GDH was less than 10 nm. According to the absorption peak for theses Au-NPs (Fig. S8D), which was detected at 535 nm, the size of the nanoparticles corresponds to a size of 50 nm according to He et al. (2005). The reason for this discrepancy lies in the fact that the spectrum was recorded in a buffered solution containing protein. It is known that the environment has an influence on the optical properties of metal nanoparticles (Kelly et al. 2003).

Supplementary Information The online version contains supplementary material available at https://doi.org/10.1007/s00253-023-12853-1.

Authors' contributions LM carried out the most experimental work, do the data processing and participate in the describing the results and drafted the manuscript. RL conceived the study, participate in its design and coordination, funding acquisition IR—Project administration, MA and DP – TEM analysis,data processing and participate in the describing the results AVP- conceived the study, participate in its design and coordination, modelling of the experimental data and drafted the manuscript.

Funding This study was funded by the Croatian Science Foundation programme Young Researchers' Career Development Project – Training of New Doctoral Students, research projects Synthesis and Targeted Application of Metallic Nanoparticles – STARS (HRZZ-UIP-2014–09-1534) and Antibacterial Coating for biodegradable medicine materials – ABBAMEDICA (HRZZ-IP-2019–04-1381), Scholarship of the Scholarship Foundation of the Republic of Austria (Undergraduates, Graduates, Postgraduates) awarded by The Austrian Agency for International Cooperation in Education & Research (OeAD-GmbH), and Croatian-Austrian bilateral project Influence of the bioavailability of metal ion sin biomass on lignocellulolytic enzymes for implementation in textile processing (BIL-HR-AUT-2018–2019) financed by the Republic of Croatia Ministry of Science and Education.

Data availability statement The authors declare that the data supporting the findings of this study are available within the paper and its Supplementary Information files. Should any raw data files be needed in another format they are available from the corresponding author upon reasonable request.

Declarations

Ethical approval This article does not contain any studies with human participants or animals performed by any of the authors.

Conflict of interests The authors declare no competing interests.

References

Adelere IA, Lateef A (2016) A Novel Approach to the Green Synthesis of Metallic Nanoparticles: The Use of Agro-Wastes, Enzymes, and Pigments. Nanotechnol Rev 5:567–587. https://doi.org/10.1515/ntrev-2016-0024

Ahmad A, Senapati S, Khan MI, Kumar R, Sastry M (2006) Extra-/Intracellular Biosynthesis of Gold Nanoparticles by an Alkalotolerant Fungus, *Trichothecium* sp. J Biomed Nanotechnol 1:47–53. https://doi.org/10.1166/jbn.2005.012

Ahmed S, Annu IS, Yudha SS (2016a) Biosynthesis of gold nanoparticles: A green approach. J Photochem Photobiol B 161:141–153. https://doi.org/10.1016/j.jphotobiol.2016.04.034

Ahmed SR, Oh S, Baba R, Zhou H, Hwang S, Lee J, Park EY (2016b) Synthesis of Gold Nanoparticles with Buffer-Dependent Variations of Size and Morphology in Biological Buffers. Nanoscale Res Lett 11:65. https://doi.org/10.1186/s11671-016-1290-3

Castro-Guerrero CF, Morales-Cepeda AB, Hernández-Vega LK, Díaz-Guillén MR (2018) Fructose-Mediated Gold Nanoparticles

Synthesis. Cogent Chem 4:1447262. https://doi.org/10.1080/23312009.2018.1447262
Castro L, Blázquez JÁ, Muñoz JÁ, González FG, Ballester A (2014) Mechanism and Applications of Metal Nanoparticles Prepared by Bio-Mediated Process. Rev Adv Sci Eng 3:199–216. https://doi.org/10.1166/rase.2014.1064
Chinnadayyala SR, Santhosh M, Singh NK, Goswami P (2015) Alcohol oxidase protein mediated in-situ synthesized and stabilized gold nanoparticles for developing amperometric alcohol biosensor. Biosens Bioelectron 69:155–161. https://doi.org/10.1016/j.bios.2015.02.015
Coronato Courrol L, de Matos RA (2016) Synthesis of Gold Nanoparticles Using Amino Acids by Light Irradiation. In: Mishra NK (ed) Catalytic Application of Nano-Gold Catalysts. IntechOpen, London, pp 83–99. https://doi.org/10.5772/63729
El-Batal AI, ElKenawy NM, Yassin AS, Amin MA (2015) Laccase production by *Pleurotus ostreatus* and its application in synthesis of gold nanoparticles. Biotechnol Rep 5:31–39. https://doi.org/10.1016/j.btre.2014.11.001
Engelbrekt C, Sørensen KH, Zhang J, Welinder AC, Jensen PS, Ulstrup J (2009) Green Synthesis of Gold Nanoparticles with Starch-Glucose and Application in Bioelectrochemistry. J Mater Chem 19:7839–7847. https://doi.org/10.1039/B911111E
Faramarzi MA, Forootanfar H (2011) Biosynthesis and characterization of gold nanoparticles produced by laccase from *Paraconiothyrium variabile*. Colloids Surf B Biointerf 87:23–27. https://doi.org/10.1016/j.colsurfb.2011.04.022
Gholami-Shabani M, Shams-Ghahfarokhi M, Gholami-Shabani Z, Akbarzadeh A, Riazi G, Ajdari S, Amani A, Razzaghi-Abyaneh M (2015) Enzymatic Synthesis of Gold Nanoparticles Using Sulfite Reductase Purified from *Escherichia Coli*: A Green Eco-Friendly Approach. Process Biochem 50:1076–1085. https://doi.org/10.1016/j.procbio.2015.04.004
Gour A, Jain NK (2019) Advances in green synthesis of nanoparticles. Artif Cells Nanomed Biotechnol 47:844–851. https://doi.org/10.1080/21691401.2019.1577878
Gupta S, Singh SP, Singh R (2015) Synergistic effect of reductase and keratinase for facile synthesis of protein-coated gold nanoparticles. J Microbiol Biotechnol 25:612–619. https://doi.org/10.4014/jmb.1411.11022
Harada M, Kizaki S (2016) Formation Mechanism of Gold Nanoparticles Synthesized by Photoreduction in Aqueous Ethanol Solutions of Polymers Using In Situ Quick Scanning X-ray Absorption Fine Structure and Small-Angle X-ray Scattering. Cryst Growth Des 16:1200–1212. https://doi.org/10.1021/acs.cgd.5b01168
Harreither W, Sygmund C, Augustin M, Narciso M, Rabinovich ML, Gorton L, Haltrich D, Ludwig R (2011) Catalytic properties and classification of cellobiose dehydrogenases from ascomycetes. Appl Environ Microbiol 77:1804–1815. https://doi.org/10.1128/AEM.02052-10
He YQ, Liu SP, Kong L, Liu ZF (2005) A study on the sizes and concentrations of gold nanoparticles by spectra of absorption, resonance Rayleigh scattering and resonance non-linear scattering. Spectrochim Acta A Mol Biomol Spectrosc 61:2861–2866. https://doi.org/10.1016/j.saa.2004.10.035
Huang H, Yang X (2004) Synthesis of polysaccharide-stabilized gold and silver nanoparticles: a green method. Carbohydr Res 339:2627–2631. https://doi.org/10.1016/j.carres.2004.08.005
Huang X, El-Sayed MA (2010) Gold Nanoparticles: Optical Properties and Implementations in Cancer Diagnosis and Photothermal Therapy. J Adv Res 1:13–28. https://doi.org/10.1016/j.jare.2010.02.002
Iravani S, Zolfaghari B (2013) Green synthesis of silver nanoparticles using *Pinus eldarica* bark extract. Biomed Res Int 2013:639725. https://doi.org/10.1155/2013/639725
Jalani NS, Zati-Hanani S, Teoh YP, Abdullah R (2018) Short Review: The Effect of Reaction Conditions on Plant-Mediated Synthesis of Silver Nanoparticles. MSF 917:145–151. https://doi.org/10.4028/www.scientific.net/msf.917.145
Kamaraj C, Karthi S, Reegan AD, Balasubramani G, Ramkumar G, Kalaivani K, Zahir AA, Deepak P, Senthil-Nathan S, Rahman MM, Md Towfiqul Islam AR, Malafaia G (2022) Green synthesis of gold nanoparticles using *Gracilaria crassa* leaf extract and their ecotoxicological potential: Issues to be considered. Environ Res 213:113711. https://doi.org/10.1016/j.envres.2022.113711
Kelly KL, Coronado E, Zhao LL, Schatz GC (2003) The Optical Properties of Metal Nanoparticles: The Influence of Size, Shape, and Dielectric Environment. J Phys Chem B 107:668–677. https://doi.org/10.1021/jp026731y
Khalilzadeh MA, Borzoo M (2016) Green synthesis of silver nanoparticles using onion extract and their application for the preparation of a modified electrode for determination of ascorbic acid. J Food Drug Anal 24:796–803. https://doi.org/10.1016/j.jfda.2016.05.004
Khan ST, Malik A, Wahab R, Abd-Elkader OH, Ahamed M, Ahmad J, Musarrat J, Siddiqui MA, Al-Khedhairy AA (2017) Synthesis and characterization of some abundant nanoparticles, their antimicrobial and enzyme inhibition activity. Acta Microbiol Immunol Hung 64:203–216. https://doi.org/10.1556/030.64.2017.004
Krishnaswamy K, Vali H, Orsat V (2014) Value-Adding to Grape Waste: Green Synthesis of Gold Nanoparticles. J Food Eng 142:210–220. https://doi.org/10.1016/j.jfoodeng.2014.06.014
Kumari M, Mishra A, Pandey S, Singh SP, Chaudhry V, Mudiam MK, Shukla S, Kakkar P, Nautiyal CS (2016) Physico-Chemical Condition Optimization during Biosynthesis lead to development of Improved and Catalytically Efficient Gold Nano Particles. Sci Rep 6:27575. https://doi.org/10.1038/srep27575
Kuppusamy P, Yusoff MM, Maniam GP, Govindan N (2016) Biosynthesis of Metallic Nanoparticles Using Plant Derivatives and Their New Avenues in Pharmacological Applications – An Updated Report. Saudi Pharm J 24:473–484. https://doi.org/10.1016/j.jsps.2014.11.013
Ma S, Ludwig R (2019) Direct Electron Transfer of Enzymes Facilitated by Cytochromes. ChemElectroChem 6:958–975. https://doi.org/10.1002/celc.201801256
Malel E, Ludwig R, Gorton L, Mandler D (2010) Localized deposition of Au nanoparticles by direct electron transfer through cellobiose dehydrogenase. Chemistry 16:11697–11706. https://doi.org/10.1002/chem.201000453
Maruyama T, Fujimoto Y, Maekawa T (2015) Synthesis of gold nanoparticles using various amino acids. J Colloid Interface Sci 447:254–257. https://doi.org/10.1016/j.jcis.2014.12.046
Menon S, Rajeshkumar S, Kumar SV (2017) A Review on Biogenic Synthesis of Gold Nanoparticles, Characterization, and Its Applications. Resour-Effic Technol 3:516–527. https://doi.org/10.1016/j.reffit.2017.08.002
Mishra A, Sardar M (2014) Alpha Amylase Mediated Synthesis of Gold Nanoparticles and Their Application in the Reduction of Nitroaromatic Pollutants. Energy Environ Focus 3:179–184. https://doi.org/10.1166/eef.2014.1077
Mountrichas G, Pispas S, Kamitsos EI (2014) Effect of Temperature on the Direct Synthesis of Gold Nanoparticles Mediated by Poly(Dimethylaminoethyl Methacrylate) Homopolymer. J Phys Chem C 118:22754–22759. https://doi.org/10.1021/jp505725v
Muguruma H, Iwasa H, Hidaka H, Hiratsuka A, Uzawa H (2017) Mediatorless Direct Electron Transfer between Flavin Adenine Dinucleotide-Dependent Glucose Dehydrogenase and Single-Walled Carbon Nanotubes. ACS Catal 7:725–734. https://doi.org/10.1021/acscatal.6b02470
Muthurasu A, Ganesh V (2016) Glucose Oxidase Stabilized Fluorescent Gold Nanoparticles as an Ideal Sensor Matrix for Dual Mode Sensing of Glucose. RSC Adv 6:7212–7223. https://doi.org/10.1039/C5RA22477B
Ovais M, Khalil AT, Ayaz M, Ahmad I, Nethi SK, Mukherjee S (2018a) Biosynthesis of Metal Nanoparticles via Microbial

Enzymes: A Mechanistic Approach. Int J Mol Sci 19:4100. https://doi.org/10.3390/ijms19124100

Ovais M, Khalil AT, Islam NU, Ahmad I, Ayaz M, Saravanan M, Shinwari ZK, Mukherjee S (2018b) Role of plant phytochemicals and microbial enzymes in biosynthesis of metallic nanoparticles. Appl Microbiol Biotechnol 102:6799–6814. https://doi.org/10.1007/s00253-018-9146-7

Ovais M, Khalil AT, Raza A, Islam NU, Ayaz M, Saravanan M, Ali M, Ahmad I, Shahid M, Shinwari ZK (2018c) Multifunctional Theranostic Applications of Biocompatible Green-Synthesized Colloidal Nanoparticles. Appl Microbiol Biotechnol 102:4393–4408. https://doi.org/10.1007/s00253-018-8928-2

Park Y, Hong YN, Weyers A, Kim YS, Linhardt RJ (2011) Polysaccharides and phytochemicals: a natural reservoir for the green synthesis of gold and silver nanoparticles. IET Nanobiotechnol 5:69–78. https://doi.org/10.1049/iet-nbt.2010.0033

Patra JK, Baek KH (2014) Green Nanobiotechnology: Factors Affecting Synthesis and Characterization Techniques. J Nanomater 2014:417305. https://doi.org/10.1155/2014/417305

Patra JK, Baek KH (2015) Novel Green Synthesis of Gold Nanoparticles Using Citrullus Lanatus Rind and Investigation of Proteasome Inhibitory Activity, Antibacterial, and Antioxidant Potential. Int J Nanomed 10:7253–7264. https://doi.org/10.2147/IJN.S95483

Rajeshkumar S, Venkat Kumar S, Malarkodi C, Vanaja M, Paulkumar K, Annadurai G (2017) Optimized Synthesis of Gold Nanoparticles Using Green Chemical Process and Its Invitro Anticancer Activity Against HepG2 and A549 Cell Lines. Mech Mater Sci Eng 9. doi: https://doi.org/10.2412/mmse.95.26.479

Rangnekar A, Sarma TK, Singh AK, Deka J, Ramesh A, Chattopadhyay A (2007) Retention of enzymatic activity of alpha-amylase in the reductive synthesis of gold nanoparticles. Langmuir 23:5700–5706. https://doi.org/10.1021/la062749e

Sanghi R, Verma P, Puri S (2011) Enzymatic Formation of Gold Nanoparticles Using *Phanerochaete Chrysosporium*. Adv Chem Eng Sci 1:154–162. https://doi.org/10.4236/aces.2011.13023

Sathiyanarayanan G, Vignesh V, Saibaba G, Vinothkanna A, Dineshkumar K, Viswanathan MB, Selvin J (2014) Synthesis of Carbohydrate Polymer Encrusted Gold Nanoparticles Using Bacterial Exopolysaccharide: A Novel and Greener Approach. RSC Adv 4:22817–22828. https://doi.org/10.1039/C4RA01428F

Scampicchio M, Fuenmayor CA, Mannino S (2009) Sugar determination via the homogeneous reduction of Au salts: a novel optical measurement. Talanta 79:211–215. https://doi.org/10.1016/j.talanta.2009.03.033

Sharma B, Mandani S, Sarma TK (2013) Biogenic growth of alloys and core-shell nanostructures using urease as a nanoreactor at ambient conditions. Sci Rep 3:2601. https://doi.org/10.1038/srep02601

Shervani Z, Yamamoto Y (2011) Carbohydrate-directed synthesis of silver and gold nanoparticles: effect of the structure of carbohydrates and reducing agents on the size and morphology of the composites. Carbohydr Res 346:651–658. https://doi.org/10.1016/j.carres.2011.01.020

Shi W, Casas J, Venkataramasubramani M, Tang L (2012) Synthesis and Characterization of Gold Nanoparticles with Plasmon Absorbance Wavelength Tunable from Visible to Near Infrared Region. ISRN Nanomater 2012:659043. https://doi.org/10.5402/2012/659043

Suvarna S, Das U, Kc S, Mishra S, Sudarshan M, Saha KD, Dey S, Chakraborty A, Narayana Y (2017) Synthesis of a novel glucose capped gold nanoparticle as a better theranostic candidate. PLoS ONE 12(6):e0178202. https://doi.org/10.1371/journal.pone.0178202

Sygmund C, Klausberger M, Felice AK, Ludwig R (2011) Reduction of quinones and phenoxy radicals by extracellular glucose dehydrogenase from *Glomerella cingulata* suggests a role in plant pathogenicity. Microbiology 157(Pt 11):3203–3212. https://doi.org/10.1099/mic.0.051904-0

Sygmund C, Kracher D, Scheiblbrandner S, Zahma K, Felice AK, Harreither W, Kittl R, Ludwig R (2012) Characterization of the two Neurospora crassa cellobiose dehydrogenases and their connection to oxidative cellulose degradation. Appl Environ Microbiol 78:6161–6171. https://doi.org/10.1128/AEM.01503-12

Sylvestre J, Poulin S, Kabashin AV, Sacher E, Meunier M, Luong JHT (2004) Surface chemistry of gold nanoparticles produced by laser ablation in aqueous media. J Phys Chem B 108:16864–16869. https://doi.org/10.1021/jp047134

Tavahodi M, Ortiz R, Schulz C, Ekhtiari A, Ludwig R, Haghighi B, Gorton L (2017) Direct Electron Transfer of Cellobiose Dehydrogenase on Positively Charged Polyethyleneimine Gold Nanoparticles. ChemPlusChem 82:546–552. https://doi.org/10.1002/cplu.201600453

Venkatpurwar VP, Pokharkar VB (2010) Biosynthesis of gold nanoparticles using therapeutic enzyme: in-vitro and in-vivo efficacy study. J Biomed Nanotechnol 6:667–674. https://doi.org/10.1166/jbn.2010.1163

Vrsalović Presečki A, Pintarić L, Švarc A, Vasić-Rački Đ (2018) Different strategies for multi-enzyme cascade reaction for chiral vic-1,2-diol production. Bioprocess Biosyst Eng 41:793–802. https://doi.org/10.1007/s00449-018-1912-5

Wang X, Falk M, Ortiz R, Matsumura H, Bobacka J, Ludwig R, Bergelin M, Gorton L, Shleev S (2012) Mediatorless sugar/oxygen enzymatic fuel cells based on gold nanoparticle-modified electrodes. Biosens Bioelectron 31:219–225. https://doi.org/10.1016/j.bios.2011.10.020

Xu JX, Siriwardana K, Zhou Y, Zou S, Zhang D (2018) Quantification of Gold Nanoparticle Ultraviolet-Visible Extinction, Absorption, and Scattering Cross-Section Spectra and Scattering Depolarization Spectra: The Effects of Nanoparticle Geometry, Solvent Composition, Ligand Functionalization, and Nanoparticle Aggregation. Anal Chem 90:785–793. https://doi.org/10.1021/acs.analchem.7b03227

Yadi M, Mostafavi E, Saleh B, Davaran S, Aliyeva I, Khalilov R, Nikzamir M, Nikzamir N, Akbarzadeh A, Panahi Y, Milani M (2018) Current developments in green synthesis of metallic nanoparticles using plant extracts: a review. Artif Cells Nanomed Biotechnol 46:S336–S343. https://doi.org/10.1080/21691401.2018.1492931

Yasui K, Kimizuka N (2005) Enzymatic Synthesis of Gold Nanoparticles Wrapped by Glucose Oxidase. Chem Lett 34:416–417. https://doi.org/10.1246/cl.2005.416

Zafar MN, Wang X, Sygmund C, Ludwig R, Leech D, Gorton L (2012) Electron-transfer studies with a new flavin adenine dinucleotide dependent glucose dehydrogenase and osmium polymers of different redox potentials. Anal Chem 84:334–341. https://doi.org/10.1021/ac202647z

Zuber A, Purdey M, Schartner E, Forbes C, Van Der Hoek B, Giles D, Abell A, Monro T, Ebendorff-Heidepriem H (2016) Detection of Gold Nanoparticles with Different Sizes Using Absorption and Fluorescence Based Method. Sens Actuators B 227:117–127. https://doi.org/10.1016/j.snb.2015.12.044